Neurotoxicology 70 (2019) 1–11

Contents lists available at ScienceDirect

Neurotoxicology

journal homepage: www.elsevier.com/locate/neuro

Full Length Article

6-Hydroxydopamine induces different mitochondrial bioenergetics response in brain regions of rat

Débora F. Gonçalves[a], Aline A. Courtes[a], Diane D. Hartmann[a], Pamela C. da Rosa[a], Débora M. Oliveira[a], Félix A.A. Soares[a], Cristiane L. Dalla Corte[a,b,*]

[a] Universidade Federal de Santa Maria, Centro de Ciências Naturais e Exatas, Departamento de Bioquímica e Biologia Molecular, Programa de Pós-graduação em Ciências Biológicas: Bioquímica Toxicológica, Camobi, 97105-900, Santa Maria, RS, Brazil
[b] Universidade Federal do Pampa - Campus Caçapava do Sul, 96570-000, Caçapava do Sul, RS, Brazil

ARTICLE INFO

Keywords:
Parkinson disease
Neurodegenerative disease
Mitochondrial function
High-resolution respirometry
ROS production

ABSTRACT

Mitochondrial dysfunction has been demonstrated to have a central role in Parkinson Disease (PD) pathophysiology. Some studies have indicated that PD causes an impairment in mitochondrial bioenergetics; however, the effects of PD on brain-region specific bioenergetics was never investigated before. This study aimed to evaluate mitochondrial bioenergetics in different rat brain structures in an *in vitro* model of PD using 6-OHDA. Rat brain slices of hippocampus, striatum, and cortex were exposed to 6-OHDA (100 μM) for 1 h and mitochondrial bioenergetic parameters, peroxide production, lactate dehydrogenase (LDH) and citrate synthase (CS) activities were analyzed. Hippocampus slices exposed to 6-OHDA presented increased peroxide production but, no mitochondrial adaptive response against 6-OHDA damage. Cortex slices exposed to 6-OHDA presented increased oxygen flux related to oxidative phosphorylation and energetic pathways exchange demonstrated by the increase in LDH activity, suggesting a mitochondrial compensatory response. Striatum slices exposed to 6-OHDA presented a decrease of oxidative phosphorylation and decrease of oxygen flux related to ATP-synthase indicating an impairment in the respiratory chain. The co-incubation of 6-OHDA with n-acetylcysteine (NAC) abolished the effects of 6-OHDA on mitochondrial function in all brain regions tested, indicating that the increased reactive oxygen species (ROS) production is responsible for the alterations observed in mitochondrial bioenergetics. The present results indicate a brain-region specific response against 6-OHDA, providing new insights into brain mitochondrial bioenergetic function in PD. These findings may contribute to the development of future therapies with a target on energy metabolism.

1. Introduction

Parkinson disease (PD) is considered the second most common neurodegenerative disorder in the world (Simuni et al., 2018). PD is characterized by loss of dopaminergic neurons and formation of protein aggregates, such as α-synuclein (Requejo-Aguilar et al., 2014), leading to motor dysfunction, and impairment of cognitive and memory functions (Goetz, 2011; Riederer et al., 2018). The pathology and symptoms of PD are well described, although its mechanisms and causes remain unclear (Goetz, 2011). One mechanism involved in PD is mitochondrial dysfunction (Ammal Kaidery and Thomas, 2018; Teves et al., 2018; Wu et al., 2018). Mutation in genes involved in mitochondrial quality control, such as PARK2 and PINK1, produce PD symptoms (Wang et al., 2011). These genes code for proteins such as PINK1 (PTEN induced kinase 1) that is a serine/threonine kinase involved in mitochondrial network quality control (Gautier et al., 2008).

Mitochondrial quality control and normal mitochondrial functionality are crucial to maintaining the cell energy balance (Lisowski et al., 2018). Investigations demonstrated that besides the impairment of mitochondrial function, PD has consequences over the energetic routes (Requejo-Aguilar et al., 2014). Observations from genetic models of the disease indicate that PD may drive an energy generation (Requejo-Aguilar and Bolaños, 2016) shift from aerobic to glycolytic route (Requejo-Aguilar et al., 2014) similar to what is observed in cancer cells (Devine et al., 2011).

Dopaminergic neurons from striatum are usually described to be affected by PD (Massari et al., 2016; Riederer et al., 2018; Zheng et al., 2018). However, the brain is constituted by different regions that are responsible for distinct functions, therefore, bioenergetics and mitochondrial response against chemical exposure, aging or

* Corresponding author at: Universidade Federal do Pampa, Campus Caçapava do Sul, 96570-000, Caçapava do Sul, RS, Brazil
E-mail address: cristianecorte@unipampa.edu.br (C.L. Dalla Corte).

https://doi.org/10.1016/j.neuro.2018.10.005
Received 6 July 2018; Received in revised form 7 October 2018; Accepted 10 October 2018
Available online 22 October 2018
0161-813X/

neurodegenerative disease may differ (Pandya et al., 2016) depending on the brain region.

In vitro models of PD are valuable tools for the investigation of mechanisms involved in the disease (Feitosa et al., 2018; Morroni et al., 2018). Analogs of dopamine, such as 6-hydroxydopamine (6-OHDA), are used both as *in vitro* and *in vivo* models of PD (Hao et al., 2017; Massari et al., 2016). Exposure to 6-OHDA mimics the PD effects like dopaminergic neurons death and increased ROS production (Lehmensiek et al., 2006). 6-OHDA was the first neurotoxin employed to cause damage specifically in neurons that use catecholamines as neurotransmitter (UNGERSTEDT, 1968) being the most used toxin in experimental PD models (Blandini et al., 2008). 6-OHDA accumulates inside neurons, promoting ROS formation (Blandini et al., 2008) and selective damage of dopaminergic/catecholaminergic neurons.

6-OHDA was also demonstrated to cause brain mitochondrial dysfunction in an *in vitro* study (Massari et al., 2016). However, there is a lack of studies focusing on 6-OHDA effects on mitochondrial bioenergetics of different brain structures. Studies about the metabolic status of individual brain regions are important for the evaluation of drugs or therapies that may target energy metabolism. Therefore, this study aimed to investigate different responses against 6-OHDA damage on mitochondrial bioenergetics function. In this way, we chose three different brain structures, cortex, hippocampus and striatum of rats, to study 6-OHDA effects. These brain regions have different concentration of dopaminergic neurons, so it is possible to predict different responses to 6-OHDA mainly in mitochondria, which play a main role in cellular response against damage.

2. Materials and methods

2.1. Chemicals

2,4,5-Trihydroxyphenethylamine hydrochloride (6-OHDA), adenosine 5′-diphosphate sodium salt (ADP), pyruvic acid, antimycin A, rotenone, malonic acid and carbonyl cyanide 4-(trifluoromethoxy)phenylhydrazone (FCCP) were purchased from Sigma-Aldrich (St. Louis, MO). Lactate dehydrogenase (LDH) commercial kit (LDH liquiform) was purchased from Labtest® Diagnostica S.A. (Minas Gerais, Brazil). Other chemicals used in this work were purchased from local suppliers.

2.2. Animals

Male adult Wistar rats (8 weeks old, 200–250 g) from our own breeding colony were maintained in a separate animal room, with light/dark cycles of 12 h each, at a temperature of 22 ± 2 °C, with free access to food and water. This study was approved by the Ethical and Animal Welfare Committee of the Federal University of Santa Maria, Brazil, under the process number 1908310517/2017.

2.3. Preparation of cerebrocortical, hippocampal and striatal slices

Animals were killed by decapitation, the brain was removed, and the cerebral cortex, hippocampus, and striatum were dissected in ice-cold Krebs–Ringer bicarbonate buffer (KRB), this buffer is compound by 136 mM NaCl, 5 mM KCl, 1.2 mM $MgSO_4$, 2.5 mM $CaCl_2$, 1.2 mM KH_2PO_4, 23.8 mM $NaHCO_3$, and 11 mM D-glucose. The buffer was bubbled with 95% O_2 – 5% CO_2 and established pH 7.4. Slices (0.4 mm) were prepared using a McIlwain Tissue Chopper (The Mickle Laboratory Engineering Co. ltd., England) and transferred to KRB buffer for 30 min at 37 °C to metabolic recover, before starting the experiments.

2.4. Slices exposure to 6-OHDA

In order to evaluate 6-OHDA toxic effects, slices were exposed for 1 h at 37 °C to 6-OHDA at a concentration of 100 μM diluted in KRB as described by a previous study (Massari et al., 2016).

2.5. Slices co-exposure to 6-OHDA and n-acetylcysteine (NAC)

To evaluate the effects of the concomitant exposure to NAC and 6-OHDA on high-resolution respirometry (HRR), brain slices were incubated for 1 h at 37 °C with 6-OHDA at a concentration of 100 μM diluted in KRB plus NAC at a concentration of 1 mM also diluted in KRB. The NAC concentration used in this assay was based on a previous study (Qian and Yang, 2009).

2.6. High-resolution respirometry (HRR)

The analyses were performed on O2k-system high-resolution oxygraph (Oroboros Instruments, Innsbruck, Austria). Cerebral structure slices were added to the chamber containing the respiration medium - MIR05 (0.5 mM EGTA, 3 mM $MgCl_2$, 60 mM lactobionic acid, 20 mM taurine, 10 mM KH_2PO_4, 20 mM HEPES, 110 mM sucrose, 0.1 mg/mL fatty acid free BSA) at 37 °C. The protocol consisted of a sequential titration of multiple substrates, uncouplers and inhibitors (SUIT protocol) as described by Figs. 1A, 2A and 3A (Pesta and Gnaiger, 2011). After signal stabilization, the experimental SUIT protocol was performed by sequential addition of pyruvate (5 mM), malate (2 mM) and glutamate (10 mM); ADP (5 mM); succinate (10 mM); oligomycin (2.5 μM); carbonyl cyanide-4-(tri-fluoromethoxy) phenylhydrazone (FCCP - titrations of 0.25 μM until reaching the maximum oxygen consumption); rotenone (0.5 μM); malonate (5 mM) and antimycin (2.5 μM) (Pesta and Gnaiger, 2011; Schöpf et al., 2016). All data related to SUIT protocol were normalized by the citrate synthase activity of each sample.

2.7. Oxygen consumption related to cytochrome c oxidase

Oxygen consumption driven by cytochrome c oxidase (mitochondrial complex IV) was evaluated based on previous protocol with some adaptations (Lemieux et al., 2017). To evaluate the effects of 6-OHDA related to complex IV driven respiration, slices of hippocampus, cortex, and striatum were placed in the oroboros chambers and substrates and inhibitor were sequentially added. Glutamate (10 mM), malate (2 mM) and succinate (10 mM), and ADP (5 mM) were added to drive a coupled state, after, potassium cyanide (KCN) was used as an inhibitor in titrations of 10 μM until reaching the concentration of 100 μM. Oxygen consumption was monitored after each KCN addition.

2.8. Hydrogen peroxide (H_2O_2) production

H_2O_2 production was measured in the Oxygraph-2k (O2k, OROBOROS Instruments, Innsbruck, Austria) using the Sensor Green of the O2k-Fluo LED2-Module for fluorescence while respiration was analyzed. The H_2O_2-sensitive probe Amplex®Red was used to measure the peroxide flux (Krumschnabel et al., 2015). Around 20 mg of the cerebral structure slices (cerebrocortical, hippocampal and striatal) were placed inside oroboros chamber containing MiR05, 10 μM Amplex® Red (AmR) and 1 U/mL horseradish peroxidase (HRP). The product of the reaction between AmR and H_2O_2, catalyzed by HRP, is fluorescent, and O2k-Fluo LED2-Module is sensitive to this fluorescence difference. Through this protocol was possible to evaluate peroxide production in different steps of the HRR with the addiction of substrates and inhibitors. Experiments were performed with sequential additions of the following substrates and inhibitors: pyruvate (5 mM), malate (2.5 mM) and glutamate (10 mM); succinate (10 mM); rotenone (0.5 μM), to evaluate reverse flow in complex I, Olygomicin (2.5 μM), FCCP (0,25 μM) and malonate (5 mM), to evaluate reverse flow in complex II. All data related to peroxide production were normalized by citrate synthase activity of samples.

2.9. Enzyme activity assays and protein determination

For determination of enzyme activities and protein content, 2 mL suspension was removed from the Oxygraph-2k chamber at the end of each experiment and stored at −80 °C until further analysis. Enzyme activities were assayed at 37 °C.

Citrate synthase activity was measured at 412 nm, recording the linear reduction of 0.1 mM 5,5'dithiobis-2-nitrobenzoic acid (ε 412: 13.6 ml·cm^{-1} µmol^{-1}) in the presence of 0.10 mM acetyl-CoA, 10 mM oxalacetic acid and 0.1 M Tris/HCl, (pH 8.1) (Lemieux et al., 2017).

Lactate dehydrogenase (LDH) activity was measured at 340 nm using the commercial kit LDH liquiform (Labtest®, Diagnostica S.A., Minas Gerais, Brazil).

Protein content was determined by Bradford's test (Bradford, 1976) using serum albumin as a standard.

2.10. Statistical analysis

Statistical analysis and figures were performed using GraphPad Prism 6. Data are expressed as the Mean ± Standard Error of Mean (S.E.M.). Data were analyzed with unpaired t-test, and $p < 0.05$ was considered statistically significant.

3. Results

3.1. Effects of 6-OHDA treatment on HRR in brain slices

The effects of 6-OHDA on HRR were analyzed in different brain regions, cortex, hippocampus, and striatum, to investigate how these brain regions are affected by the neurotoxin. HRR data have five different states (Figs. 1A, 2A and 3A): pyruvate, glutamate, malate (PMG) related to oxygen flux without ADP; oxidative phosphorylation (OXPHOS) state that is related to oxygen flux in saturated ADP concentrations; LEAK representing oxygen flux in presence of oligomycin; electron transfer system (ETS) which is related to oxygen flux in presence of FCCP as uncoupler; and oxygen residual (ROX) which is related to oxygen flux in presence of antimycin. In addition, the ratios between oxygen flux, ETS CI/ETS CI&CII and ETS CII /ETS CI&CII, clarifies the dependent oxygen flux linked to each complex (CI e CII) in ETS state.

It was observed that exposure to 6-OHDA has different effects depending on the brain structure. In the striatum, 1 h-exposure to 6-OHDA caused a significant decrease of 46% in OXPHOS CII-Linked oxygen consumption, a decreased of around 35% in OXPHOS CI&CII-Linked oxygen consumption and a decreased of 33% in oxygen consumption linked to the LEAK state (Fig. 1A). Moreover, there was a significant increase in ETS CI/ETS CI&CII ratio in striatum exposed to 6-OHDA when compare to control group (Fig. 1B). Although, there was no significant difference in striatum ETS CII /ETS CI&CII ratios between control and 6-OHDA groups (Fig. 1C).

On the other hand, hippocampus slices exposed to 6-OHDA presented a significant increase of 98% in basal oxygen flux demonstrated by PMG levels (Fig. 2A). In addition, there was a significant increase of 62,1% in oxygen consumption drive by OXPHOS CI-linked in hippocampus slices exposed to 6-OHDA. In the same way, it was possible to verify an increase in oxygen flux (about 200%) in ROX state after 6-OHDA exposure in hippocampus brain slices. The ROX state can be associated with the ROS released by mitochondria. Concerning ETS CI/ETS CI&CII and ETS CII /ETS CI&CII ratios, there was no significant difference between control and 6-OHDA groups in the hippocampus (Fig. 2B and C).

In cortex slices exposed to 6-OHDA, it was possible to verify a significant increase of 60% in OXPHOS CII-Linked oxygen consumption. In the same way, the oxygen flux increased about 87% in OXPHOS CI&CII Linked (Fig. 3A), and an increase of 49% in ETS CII-Linked in slices exposed to 6-OHDA (Fig. 3A). Besides, there was an increase in oxygen flux of 100% in the ROX state, which is associated with increased ROS production. ETS CI/ETS CI&CII and ETS CII /ETS CI&CII ratios were not significantly affected by 6-OHDA in the cortex (Fig. 3B and C).

3.2. Effects of 6-OHDA on oxygen flux related to cytochrome c oxidase in brain slices

There were no significant effects on oxygen consumption driven by mitochondrial complex IV in brain slices in response to 6-OHDA exposure. The titration with cyanide, until the final concentration of 100 µM, decreased oxygen consumption around 50%, both in control group and 6-OHDA group in striatum (Fig. 4A), hippocampus (Fig. 4B) and cortex (Fig. 4C) brain slices.

3.3. Effects of 6-OHDA on peroxide production in brain slices

Peroxide production was evaluated in brain slices using the fluorescent probe Amplex® Red. There was an increase of 280% in peroxide production in striatum brain slices exposed to 6-OHDA when compared with the control group (Fig. 5A). At the same time, striatum slices exposed to 6-OHDA presented a decrease of 54,53% in peroxide production induced by reverse flow related to CI−Q junction (Fig. 5B).

Hippocampus slice exposed to 6-OHDA presented a significant increase of 292% in peroxide production compared to the control group (Fig. 5C). However, there was no significant difference in peroxide production related to reverse flow in CI−Q junction (Fig. 5D).

Cortex brain slices exposed to 6-OHDA presented a significant increase of 227% in peroxide production (Fig. 5E). Nevertheless, 6-OHDA exposure did not induce any significant alteration in cortex slices peroxide production related to reverse flow in CI-Q junction (Fig. 5F).

The peroxide production linked to reverse flow is associated with mitochondrial peroxide release after rotenone inhibition. We aimed to demonstrate the complex I capacity of electron transfer through the Q-junction. The amount of peroxide formed after inhibition is strongly associated with the complex I capacity to carry electrons through mitochondrial respiratory chain before inhibition. For example, a decrease in peroxide formation after rotenone inhibition in slices treated with 6-OHDA indicates an impairment in CI.

3.4. Effects of 6-OHDA on citrate synthase and lactate dehydrogenase activities in brain slices

Exposure to 6-OHDA significantly increased lactate dehydrogenase activity in cortex brain slices (Fig. 6F) but, had no effect on citrate synthase activity (Fig. 6E). On the other hand, there were no significant alterations on citrate synthase and lactate dehydrogenase activities in hippocampus and striatum brain slices after 6-OHDA exposure (Fig. 6C and D and Fig. 6A and B).

3.5. Effects of co-exposure to 6-OHDA and NAC on HRR

In order to test if the increase in ROX respiration observed in HRR experiments was a result of 6-OHDA exposure, we performed an assay using NAC as an antioxidant. Brain slices were co-incubated with 6-OHDA and NAC and the HRR parameters were evaluated. Co-exposure to 6-OHDA and NAC did not cause any significant alteration in HRR parameters in striatum (Fig. 7A), hippocampus (Fig. 7B) and cortex (Fig. 7C) when compared to the control. These results support the hypothesis that the alterations caused by 6-OHDA on mitochondrial function are related to ROS production.

4. Discussion

The different regions of the brain are responsible for distinct behaviors and actions. For instance, frontal cortex is responsible to decision, planning and judgment, hippocampus is responsible to memory, emotion and learning, and striatum is responsible to movement and

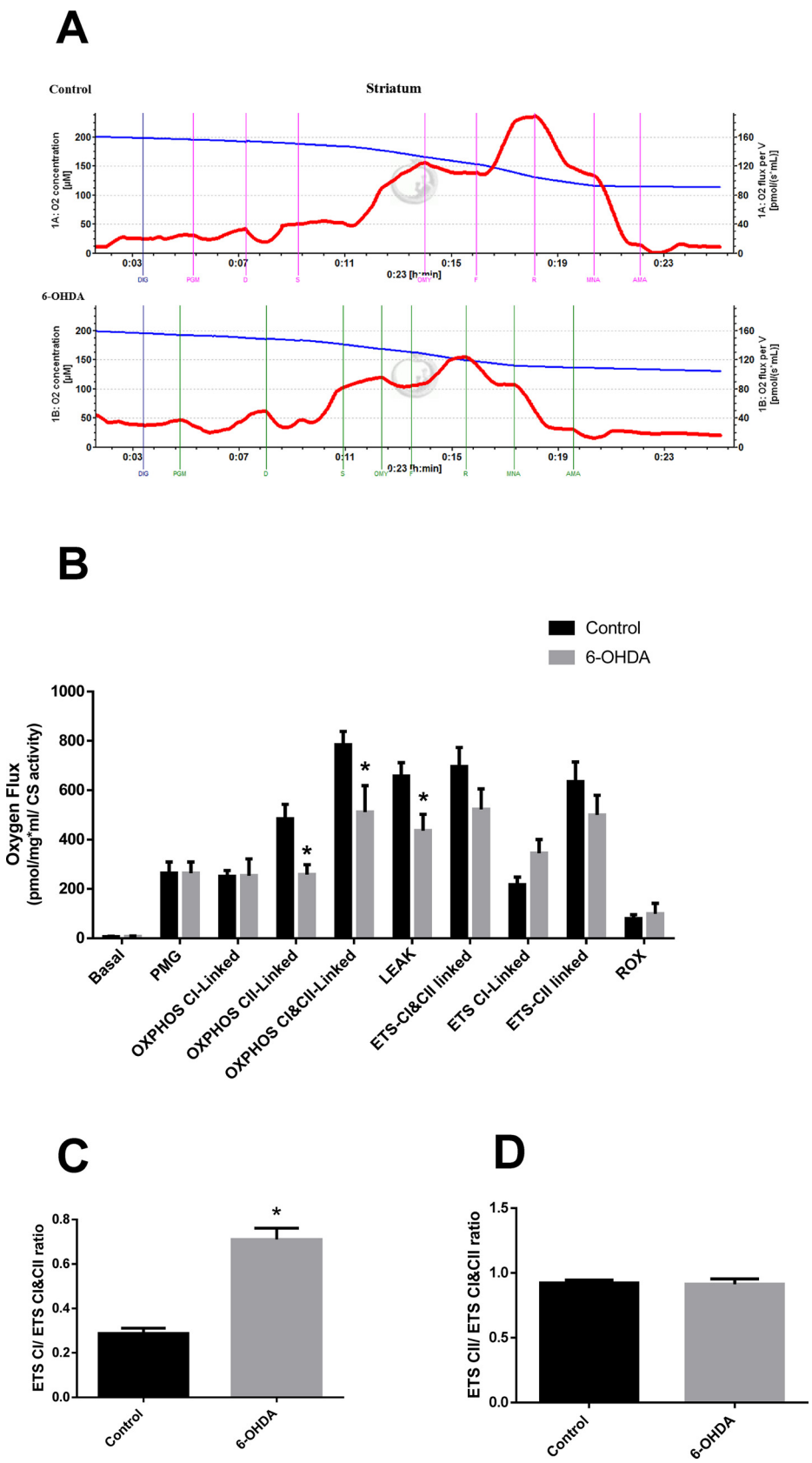

Fig. 1. Effects of 6-OHDA exposure in striatal brain slices HRR. (A) Oxygen consumption of high resolution respirometry (HRR) protocol by oroboros. Blue line represents oxygen concentration inside to oroboros chambers and red line represents electron transfer related to oxygen flux response to different substrates addition. (B) SUIT protocol result: Basal is the state without any substrates. Pyruvate, glutamate and malate were used to evaluate oxygen flux without phosphorylation (PMG). OXPHOS represents coupled states dependent on different mitochondrial substrates, pyruvate, glutamate, malate (OXPHOS CI-Linked) and succinate (OXPHOS CII-Linked and OXPHOS CI&CII-Linked) in presence of saturated ADP concentrations. LEAK is the state related to ATP-synthase inhibition by oligomicin. ETS represents maximum oxygen consumption by addition of the uncoupler FCCP (ETS CI&CII-Linked), in sequence it is demonstrated the maximum oxygen consumption related to the complex I inhibitor rotenone (ETS CI-Linked) and maximum oxygen consumption related to complex II inhibition by malonate (ETS CII-Linked), lastly, antimycin was used to inhibit complex III obtaining oxygen residual flux (ROX). (C) Ratio of values obtained in ETS CI divided by values obtained in ETS CI&CII. (D) Ratio of values obtained in ETS CII divided by values obtained in ETS CI&CII. Data are reported as mean ± S.E.M., n = 4–5. *Indicates $p < 0.05$ as compared to the control group (For interpretation of the references to colour in this figure legend, the reader is referred to the web version of this article).

cognition (Pandya et al., 2016; Zheng et al., 2018). These different functional roles played by the brain regions require appropriated energetic demands. In this way, mitochondrial metabolism and bioenergetics, may not be equal among brain regions, especially when brain is subject to impairment by drugs, aging, metabolic syndrome or neurodegenerative diseases (da Silva et al., 2012; Etchegoyen et al., 2018; Pandya et al., 2016).

Mitochondria are central regulators of energy and cell homeostasis

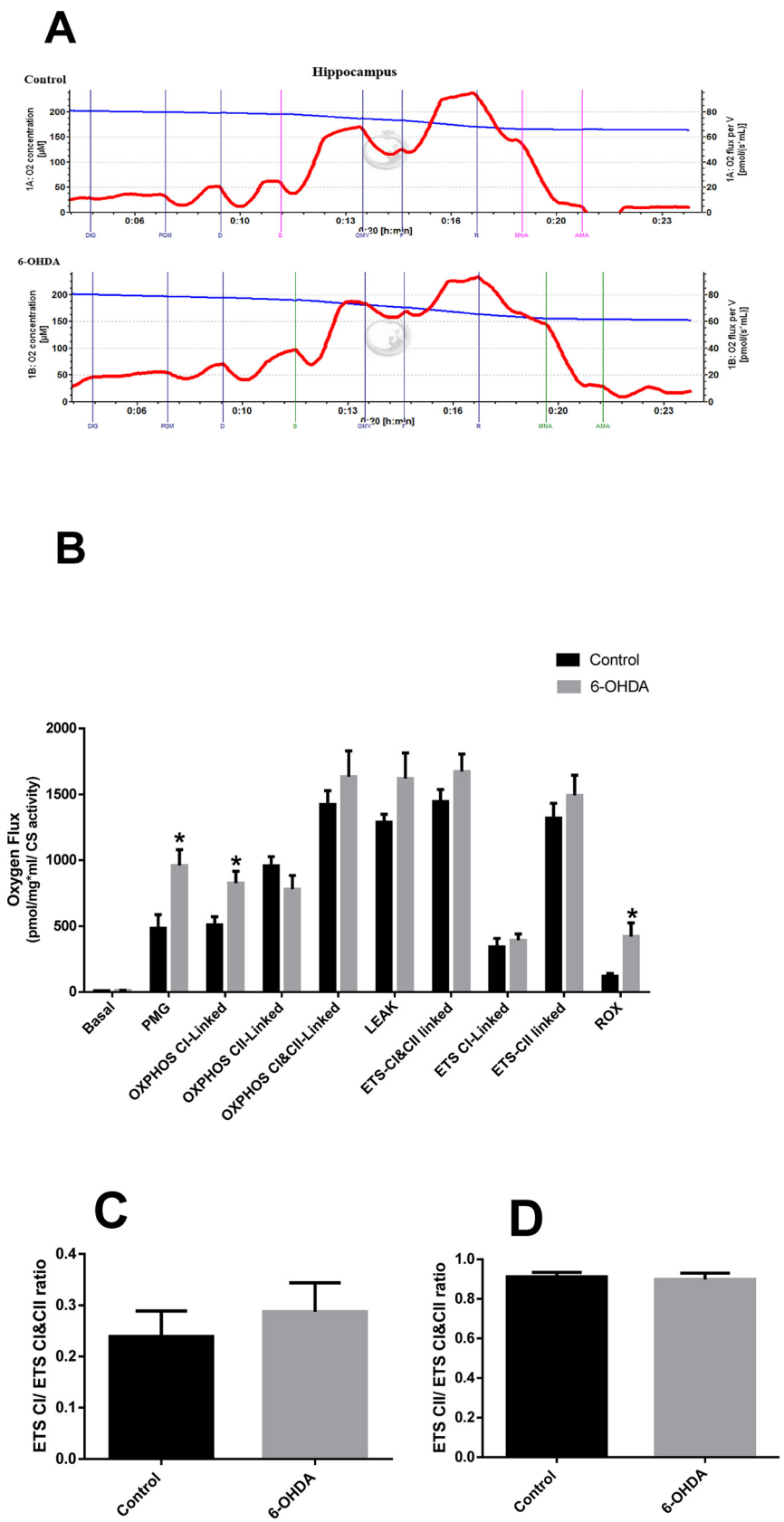

Fig. 2. Effects of 6-OHDA exposure in hippocampus brain slices HRR. (A) Oxygen consumption of high resolution respirometry (HRR) protocol by oroboros. Blue line represents oxygen concentration inside to oroboros chambers and red line represents electron transfer related to oxygen flux response to different substrates addition. (B) SUIT protocol result: Basal is the state without any substrates. Pyruvate, glutamate and malate were used to evaluate oxygen flux without phosphorylation (PMG). OXPHOS represents coupled states dependent on different mitochondrial substrates, pyruvate, glutamate, malate (OXPHOS CI-Linked) and succinate (OXPHOS CII-Linked and OXPHOS CI&CII-Linked) in presence of saturated ADP concentrations. LEAK is the state related to ATP-synthase inhibition by oligomicin. ETS represents maximum oxygen consumption by addition of the uncoupler FCCP (ETS CI&CII-Linked), in sequence it is demonstrated the maximum oxygen consumption related to the complex I inhibitor rotenone (ETS CI-Linked) and maximum oxygen consumption related to complex II inhibition by malonate (ETS CII-Linked), lastly, antimycin was used to inhibit complex III obtaining oxygen residual flux (ROX). (C) Ratio of values obtained in ETS CI divided by values obtained in ETS CI&CII. (D) Ratio of values obtained in ETS CII divided by values obtained in ETS CI&CII. Data are reported as mean ± S.E.M., n = 4–5. *Indicates $p < 0.05$ as compared to the control group (For interpretation of the references to colour in this figure legend, the reader is referred to the web version of this article).

and evidences support the critical role of mitochondrial dysfunction in neurodegenerative diseases, such as PD (Féger et al., 2002; Gautier et al., 2008; Requejo-Aguilar and Bolaños, 2016). Some studies compared PD effects in different brain regions (Massari et al., 2016; Romuk et al., 2017), although, the effects of PD on mitochondrial bioenergetics in brain regions was never investigated before. The stressors and diseases may target mitochondria energy metabolism in distinct ways with respect to different structures of the brain. Therefore, the understanding

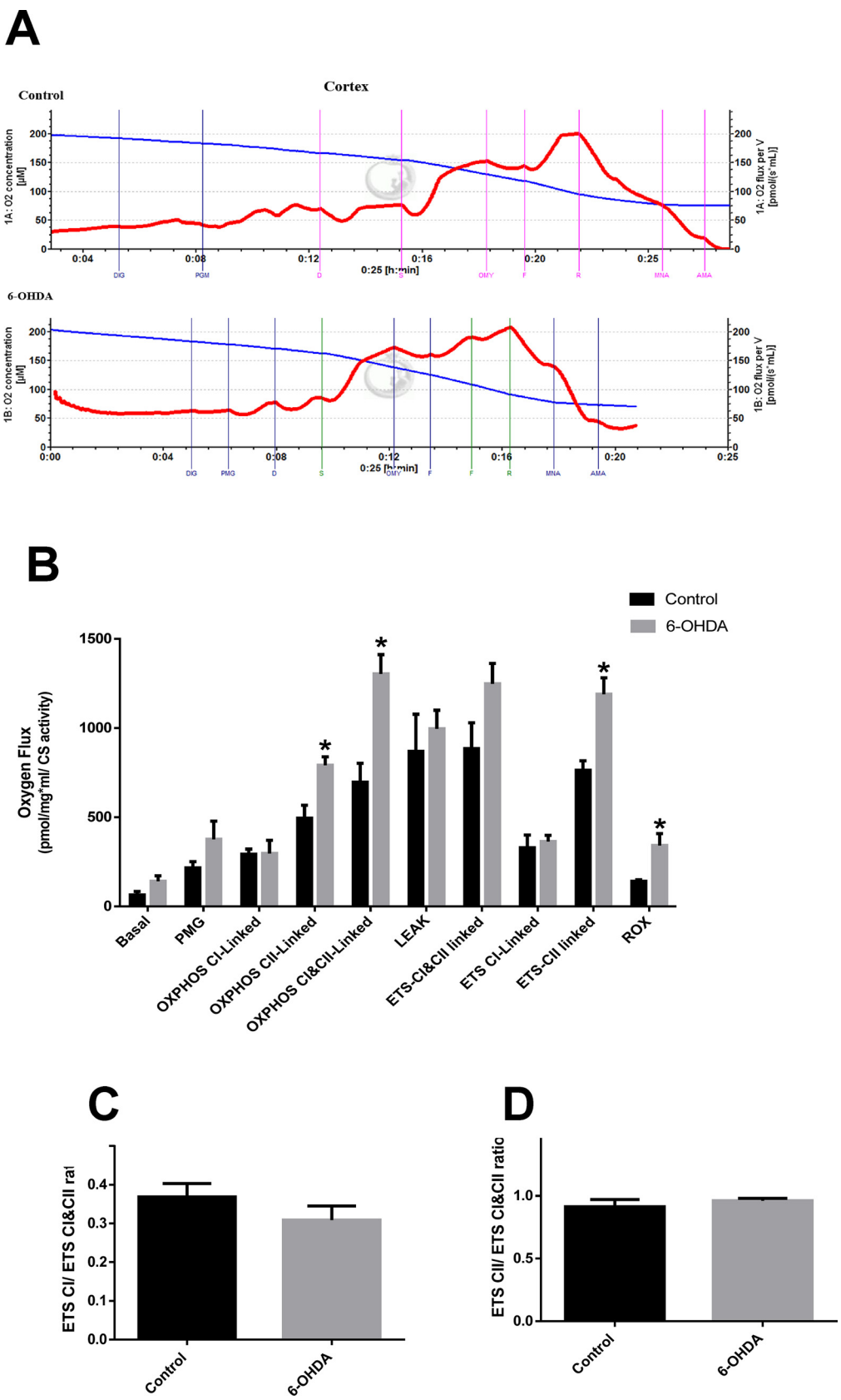

Fig. 3. Effects of 6-OHDA exposure in cortical brain slices HRR. (A) Oxygen consumption of high resolution respirometry (HRR) protocol by oroboros. Blue line represents oxygen concentration inside to oroboros chambers and red line represents electron transfer related to oxygen flux response to different substrates addition. (B) SUIT protocol result: Basal is the state without any substrates. Pyruvate, glutamate and malate were used to evaluate oxygen flux without phosphorylation (PMG). OXPHOS represents coupled states dependent on different mitochondrial substrates, pyruvate, glutamate, malate (OXPHOS CI-Linked) and succinate (OXPHOS CII-Linked and OXPHOS CI&CII-Linked) in presence of saturated ADP concentrations. LEAK is the state related to ATP-synthase inhibition by oligomicin. ETS represents maximum oxygen consumption by addition of the uncoupler FCCP (ETS CI&CII-Linked), in sequence it is demonstrated the maximum oxygen consumption related to the complex I inhibitor rotenone (ETS CI-Linked) and maximum oxygen consumption related to complex II inhibition by malonate (ETS CII-Linked), lastly, antimycin was used to inhibit complex III obtaining oxygen residual flux (ROX). (C) Ratio of values obtained in ETS CI divided by values obtained in ETS CI&CII. (D) Ratio of values obtained in ETS CII divided by values obtained in ETS CI&CII. Data are reported as mean ± S.E.M., n = 4–5. *Indicates $p < 0.05$ as compared to the control group. (For interpretation of the references to colour in this figure legend, the reader is referred to the web version of this article).

of the mitochondrial role in neurodegenerative diseases and how it modifies metabolic brain conditions in the different brain regions are important issues to be addressed (Bulteau et al., 2017; Karbowski, 2007).

In this work, we used an *in vitro* PD model with 6-OHDA to study the mitochondrial bioenergetics function in brain slices of cortex, hippocampus, and striatum. 6-OHDA is a neurotoxic compound molecularly similar to the neurotransmitter dopamine, which means that 6-OHDA

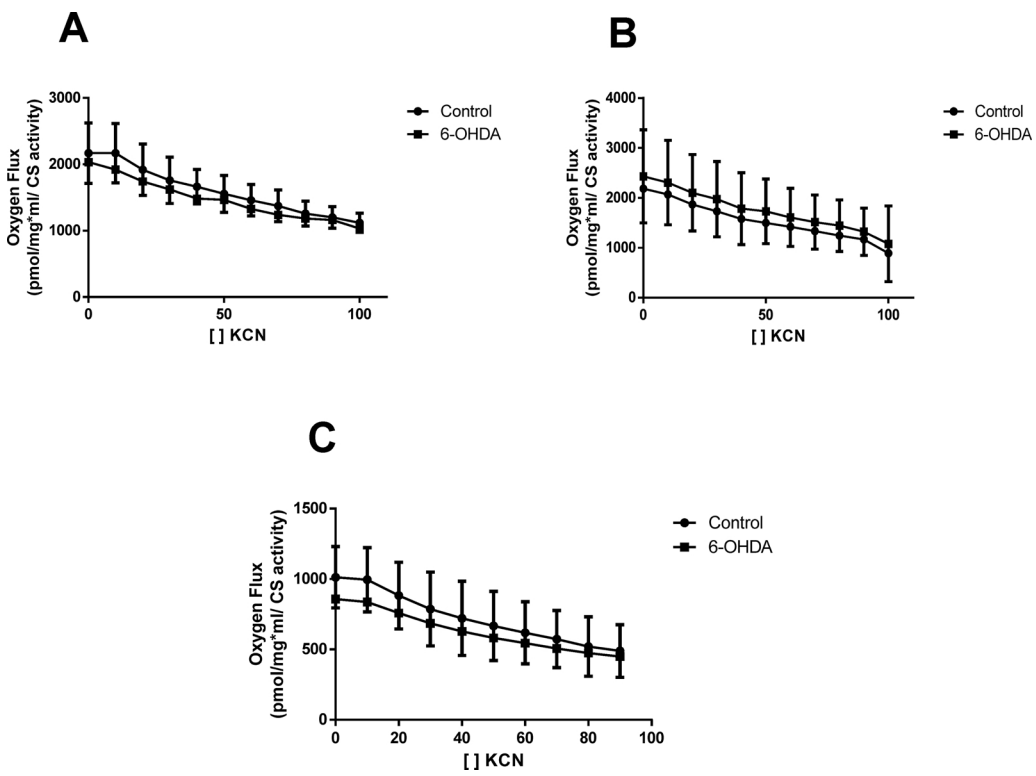

Fig. 4. Effects of 6-OHDA exposure in cytochrome c oxidase. Oxygen flux drive by cytochrome c oxidase activity in brain slices of striatum (A), hippocampus (B) and cortex (C). Potassium cyanide (KCN) was used as inhibitor of cytochrome c oxidase. We used KCN titrations of 10 μM, each value of titration in X axis corresponds to oxygen flux in Y axis. Data are reported as mean ± S.E.M of 4 different assays.

manly affects dopaminergic neurons mimicking some PD symptoms (Massari et al., 2016). Our results indicate distinct mitochondrial responses among the different brain regions due to 6-OHDA insult.

In the hippocampus it was not observed significant changes in mitochondrial functionality after 1 h of exposure to 6DA since oxygen flux in the OXPHOS CI&CII-Linked was not altered. However, 6-OHDA induced an increase in oxygen consumption related to mitochondrial proton leak, observed after PMG addition (Fig. 2A), and ROX state (Fig. 2A) which is associated with increased ROS levels. Indeed, as evidenced by the assay with Amplex® Red, hippocampus exposed to 6-OHDA presented increased peroxide production (Fig. 5C). The fact that exposure to 6-OHDA did not affect enzymatic activities of CS and LDH (Fig. 6C and D) in hippocampus slices suggest that 6-OHDA effects on hippocampus do not generate compensatory or adaptive mitochondrial response due to augmented ROS generation. When we exposed hippocampus slices to 6-OHDA associated with NAC there were no differences in mitochondrial parameters evaluated by HRR (Fig. 7B). This result indicates that 6-OHDA effects on hippocampus brain slices are mainly related to increased ROS production

Previous study demonstrated that the hippocampus is the brain structure in rats most impaired during aging (Pandya et al., 2016). Moreover, the hippocampus is important in memory formation and learning (Teixeira et al., 2018; Velazquez et al., 2018), which are abilities early affected in PD (GOETZ, 2011; Kalia and Lang, 2015). Our results corroborate these observations since the reduced mitochondrial adaptability would render the hippocampus more susceptible to ROS production and damage resulting in impaired function when treated with 6-OHDA.

On the other side, cortex slices exposed to 6-OHDA presented mitochondrial compensatory effects or adaptation perhaps as an attempt to generate energy. This hypothesis is sustained by results of oxygen flux related to oxidative phosphorylation since, after 1 hour of exposure to 6-OHDA, brain cortex slices presented an increase in oxygen flux through OXPHOS CI&CII-Linked and ETS CII-Linked (Fig. 3A). Additionally, there was a significant increase in cortical LDH activity after exposure to of 6-OHDA (Fig. 6F), reinforcing the idea of mitochondrial adaptation to increase energy generation. Lactate is an important energy source during ischemia and has been considered necessary for neuronal signaling and plasticity (Magistretti and Allaman, 2018).

The association of 6-OHDA and NAC in cortex brain slices prevented 6-OHDA effects on HRR parameters (Fig. 7C), supporting the idea that in cortex, ROS production is capable to initiate a survival signaling pathway. An increase in ROS production can lead to activation of several survival pathways, one of them is related to activation of the hypoxia-inducible factor (HIF) which is an important transcription factor that regulates cellular metabolism and cell survival under hypoxic stress (Trachootham et al., 2008). HIF plays a major role in metabolic energy source by exchanging glucose metabolites from mitochondrial respiration to cytosolic glycolysis. This metabolic exchange to the glycolytic pathway increases lactate levels (Lu et al., 2002). It is possible that in the cortex, after 1 h of 6-OHDA exposure, ROS levels increase could activate HIF explaining, in this way, the increase in LDH levels.

Based on our evidences and other studies (Devine et al., 2011; Requejo-Aguilar et al., 2014; Requejo-Aguilar and Bolaños, 2016), we believed that cortex slices exposed to 6-OHDA activates a mitochondrial compensatory effect to generate energy which is demonstrated by the increase in oxygen flux and by the exchange to other energy sources, such as lactate, demonstrated by increased LDH activity.

Moreover, the exchange of metabolic pathways to generate energy has been demonstrated in diseases such as PD (Requejo-Aguilar and Bolaños, 2016; Wang et al., 2011). The energetic pathway exchange of mitochondrial oxidative phosphorylation to a glycolytic energy source (Requejo-Aguilar et al., 2014) was previously described in PD and in cancer cells (Devine et al., 2011). Previous study indicated that in a normal situation there is a minimal mitochondrial energetic response difference among different brain regions isolated from rat brain (Sauerbeck et al., 2011). Contrariwise, other study demonstrated differences in regional brain metabolism, with evidence that the cortex seems to spend more energy than others brain regions (Karbowski, 2007). Moreover, the highest levels of aerobic glycolysis in the normal human brain reside in cortical systems. The explanation for this different metabolism has been associated with the cortex role of organization of the brain functions (Vaishnavi et al., 2010).

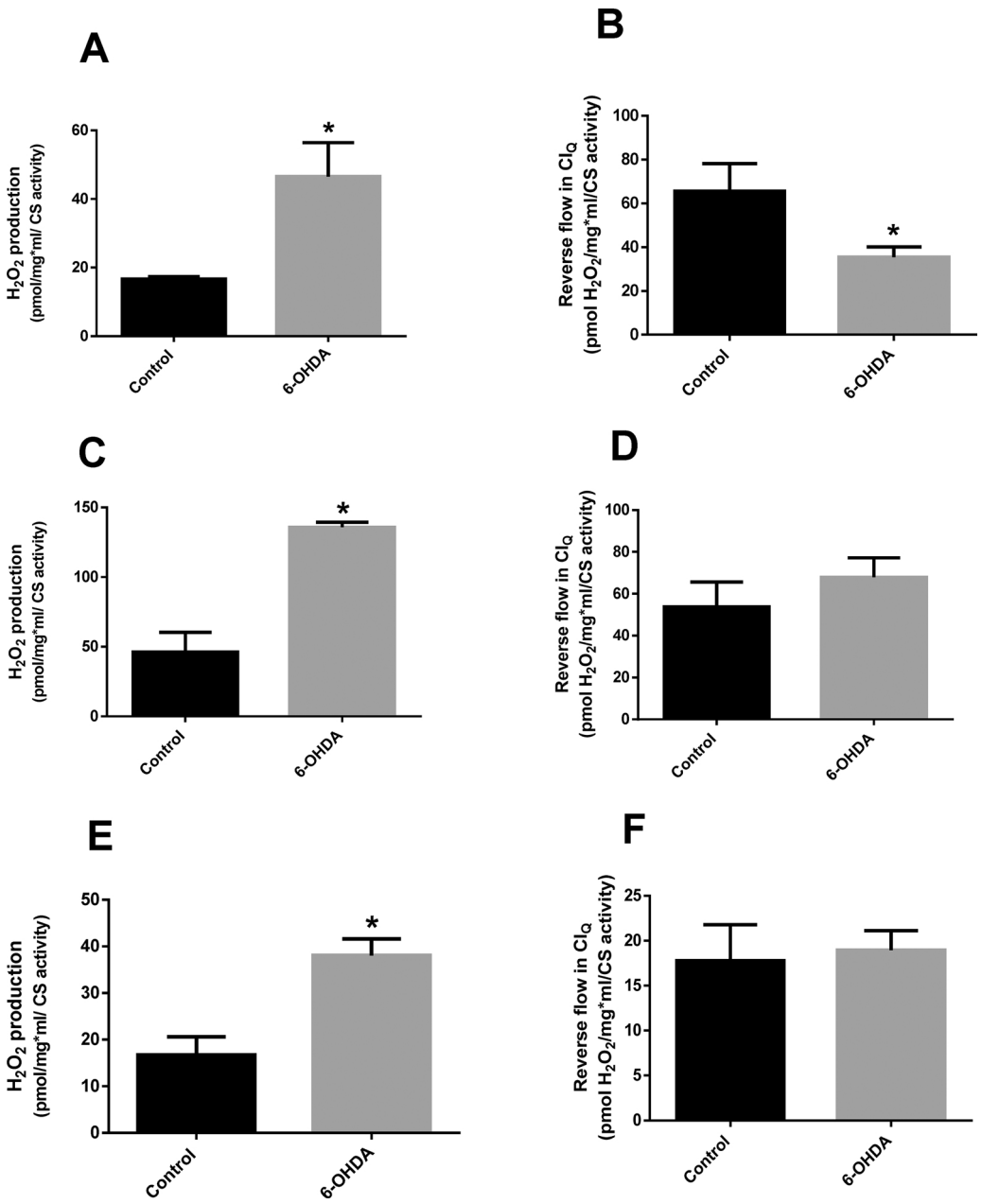

Fig. 5. Effects of 6-OHDA in brain slices peroxide production. Endogenous peroxide production, without substrates addition in striatum (A), hippocampus (C) and cortex (E) brain slices. Peroxide production by reverse flow related to CI—Q junction in striatum (B), hippocampus (D) and cortex (F) brain slices, determined by addition of substrates related to complex I (pyruvate, glutamate and malate) and complex II (succinate) and CI inhibitor rotenone. Data are reported as mean ± S.E.M., n = 4. *Indicates $p < 0.05$ as compared to the control group.

Furthermore, cortical slices exposed to 6-OHDA presented an increase in peroxide production (Fig. 5E) when compared to the control group. This increase in peroxide production in cortex after exposure to 6-OHDA was less pronounced than other brain regions tested in this work. According to other studies, ROS may promote cellular adaptations to stress conditions, by the regulation of oxidative metabolism supporting cell survival (Gutteridge and Halliwell, 2018; Makrecka-Kuka et al., 2015; Radak et al., 2016).

Even though 6-OHDA exposure increased the peroxide production in the striatum (Fig. 5A), which is in accordance with other studies (Ammal Kaidery and Thomas, 2018; Li et al., 2014; Massari et al., 2016), striatum showed a different response when compared to cortex. Different from cortex, it seems that striatum does not present any mitochondrial adaptation response against 6-OHDA damage. The increase of peroxide production in striatum slices treated with 6-OHDA was 280% higher than control (Fig. 5A). We believe that this high peroxide production in striatum was able to cause mitochondrial damage instead to mitochondrial adaptation.

Moreover, 6-OHDA exposure in striatum also induced a significant decrease in reverse flow linked to CI-Q junction after rotenone addition (Fig. 5B). This decrease in peroxide levels related to reverse flow may indicate that the general increase in peroxide production (Fig. 5A) was not caused by reverse electron flow in CI-Q junction. We believe that the amount of peroxide production in the striatum after 6-OHDA exposure could be linked to extramitochondrial cellular compartments. It was demonstrated previously that mitochondrial and cytosolic ROS formation have opposing effects on lifespan, the mitochondrial ROS formation was able to increase lifespan in Caenorhabditis elegans probably by activating cellular survival pathways, on the other hand, cytosolic ROS formation did not present the same effect in lifespan,

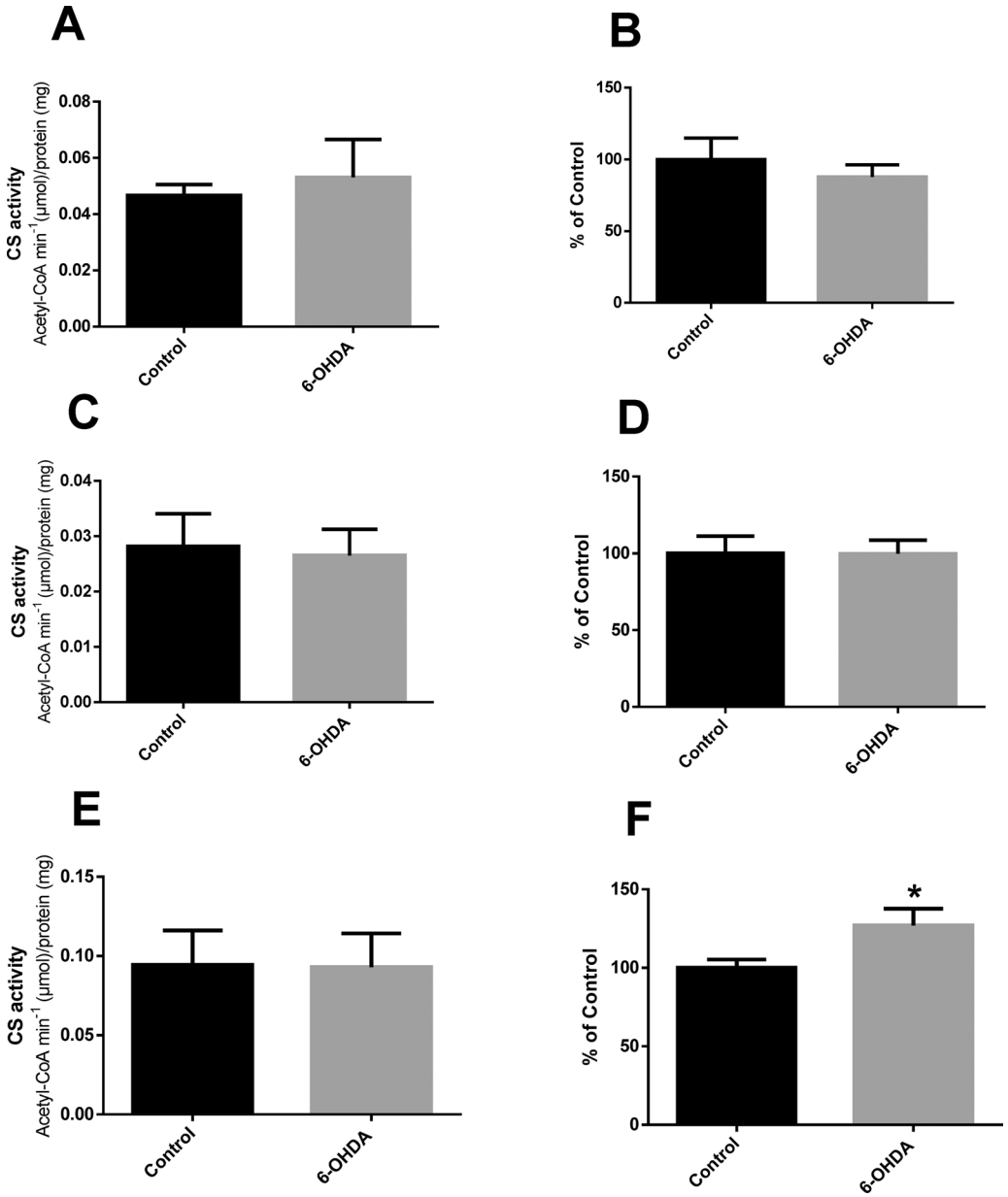

Fig. 6. Effects of 6-hydroxydopamine (6-OHDA) exposure in citrate synthase activity of striatal (A), hippocampus (C) and cortex (E) brain slices and, in lactate dehydrogenase activity of striatum (B), hippocampus (D) and cortex (F). Data are reported as mean ± S.E.M., n = 7.

(Schaar et al., 2015).

The striatum is normally the brain region more affected by 6-OHDA due to the higher number of dopaminergic neurons which are the main targets of this neurotoxin. The same occurs in PD, with striatum being the brain region most affected by the loss of dopaminergic neurons (Féger et al., 2002; Hawlitschka and Wree, 2018). In agreement with this, our results showed that striatum slices exposed to 6-OHDA presented a decrease in oxygen flux related OXPHOS CI&CII-Linked (Fig. 1) and oxygen flux related to ATP-synthase represented by the LEAK state (Fig. 1) indicating a decrease in mitochondrial functionality. Additionally, the ETS ratio evidenced an increase in CI participation on ETS state in the striatum after 6-OHDA exposure. We believe that this result is related to a decrease in mitochondrial excess capacity. Co-exposure with NAC abolished 6-OHDA effects in striatal slices most probably due to NAC antioxidant properties (Fig. 7A). At the same time, 6-OHDA exposure did not cause alterations in CS and LDH activities (Fig. 6A and B) in striatum, suggesting that this brain region cannot adapt to 6-OHDA damage.

Similarly, another work (Singh et al., 2010) demonstrated that striatal neurons exposed to 3-nitropropionic acid showed a higher mitochondrial vulnerability than cortical neurons, indicating a different energetic response against injury. Additionally, it was suggested that in neurodegenerative disease, specific nervous system components or brain regions appear to be more susceptible to the pathological process triggering. Such specific susceptibility of the brain regions to different kinds of injury is related to cell metabolism and differences in mitochondrial capacity to produce energy (Dubinsky, 2009)

5. Conclusion

In conclusion, our study demonstrated the different response related to mitochondrial bioenergetics in distinct brain regions after exposure to 6-OHDA *in vitro*. Brain regions have different metabolism and respond in different ways to 6-OHDA toxicity. The findings of this work are important to understand how mitochondrial function in the different brain regions is affected in a model of PD induced by 6-OHDA,

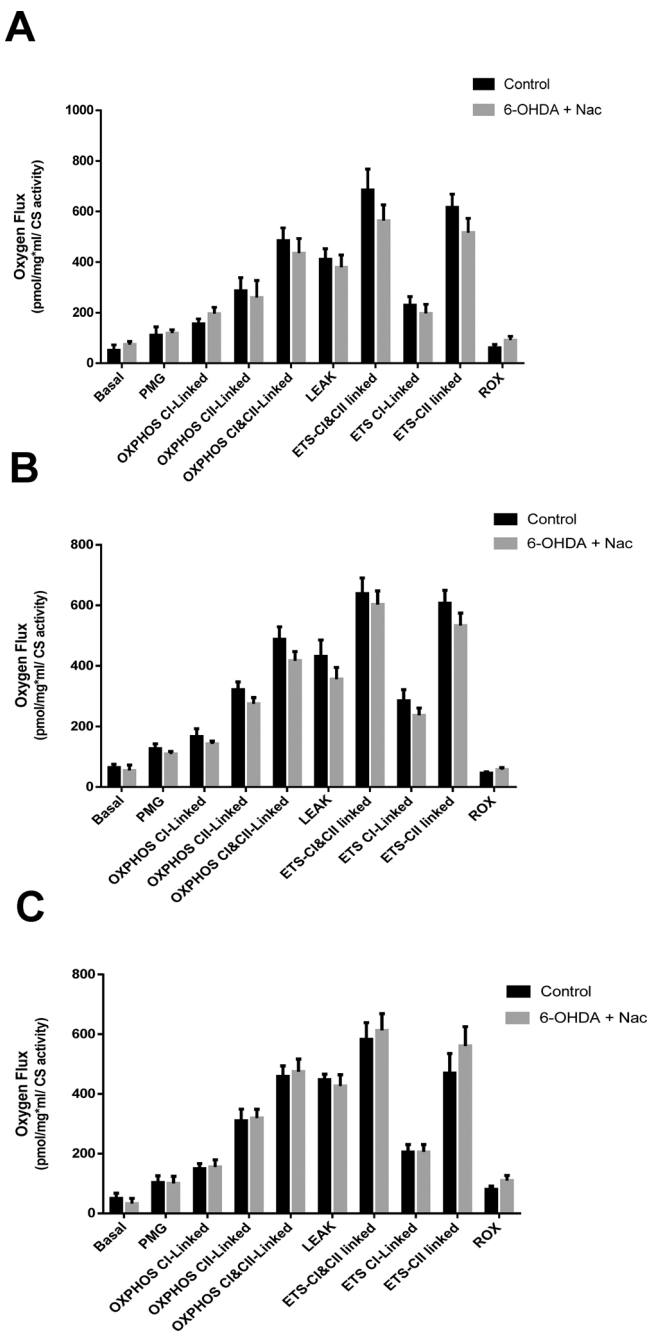

Fig. 7. Effects of 6-OHDA and NAC co-exposure in striatum (A) hippocampus (B) and cortex (C) brain slices HRR. SUIT protocol result: Basal is the state without any substrates. Pyruvate, glutamate and malate were used to evaluate oxygen flux without phosphorylation (PMG). OXPHOS represents coupled states dependent on different mitochondrial substrates, pyruvate, glutamate, malate (OXPHOS CI-Linked) and succinate (OXPHOS CII-Linked and OXPHOS CI&CII-Linked) in presence of saturated ADP concentrations. LEAK is the state related to ATP-synthase inhibition by oligomicin. ETS represents maximum oxygen consumption by addition of the uncoupler FCCP (ETS CI&CII-Linked), in sequence it is demonstrated the maximum oxygen consumption related to the complex I inhibitor rotenone (ETS CI-Linked) and maximum oxygen consumption related to complex II inhibition by malonate (ETS CII-Linked), lastly, antimycin was used to inhibit complex III obtaining oxygen residual flux (ROX). Data are reported as mean ± S.E.M., n = . 4–5.

expanding the knowledge about the involvement of mitochondrial brain metabolism in experimental PD models.

Funding

Financial support for this study was provided by Fundação de Amparo à pesquisa do Estado do RS (FAPERGS), Brazilian National Council of Technological and Scientific Development (CNPq), Coordenação de Aperfeiçoamento de Pessoal de Nível Superior (CAPES), Brazilian National Institute for Science and Technology (INCT), "Programa de Apoio a Núcleos Emergentes" (PRONEM) and MCTI/CNPq [grant numbers 472669/2011-7, 475896/2012-2]. Programa de excelência acadêmica (PROEX) process number 88882.182139/2018-01.

References

Ammal Kaidery, N., Thomas, B., 2018. Current perspective of mitochondrial biology in Parkinson's disease. Neurochem. Int. 117 (14 march) 91-117.
Blandini, F., Armentero, M.-T., Martignoni, E., 2008. The 6-hydroxydopamine model: news from the past. Parkinsonism Relat. Disord. 14 (Suppl. 2), S124–9.
Bradford, M.M., 1976. A rapid and sensitive method for the quantitation of microgram quantities of protein utilizing the principle of protein-dye binding. Anal. Biochem. 72, 248–254 7 maio.
Bulteau, A.-L., et al., 2017. Dysfunction of mitochondrial Lon protease and identification of oxidized protein in mouse brain following exposure to MPTP: implications for Parkinson disease. Free Radic. Biol. Med. 108 (30 July), 236–246.
Da Silva, M.H., et al., 2012. Acute brain damage induced by acetaminophen in mice: effect of diphenyl diselenide on oxidative stress and mitochondrial dysfunction. Neurotox. Res. 21 (3), 334–344 abr.
Devine, M.J., Plun-Favreau, H., Wood, N.W., 2011. Parkinson's disease and cancer: two wars, one front. Nat. Rev. Cancer 11 (11), 812–823 24 out.
Dubinsky, J.M., 2009. Heterogeneity of nervous system mitochondria: location, location, location!. Exp. Neurol. 218 (2), 293–307 ago.
Etchegoyen, M., et al., 2018. Metabolic syndrome and neuroprotection. Front. Neurosci. 12, 196 20 abr.
Féger, J., et al., 2002. Experimental models of Parkinson's disease. Ann. Pharm. Fr. 60 (january 1), 3–21.
Feitosa, C.M., et al., 2018. Determination of parameters of oxidative stress in vitro models of neurodegenerative diseases-a review. Curr. Clin. Pharmacol. 13 (1 March).
Gautier, C.A., Kitada, T., Shen, J., 2008. Loss of PINK1 causes mitochondrial functional defects and increased sensitivity to oxidative stress. Proc. Natl. Acad. Sci. 105 (32), 11364–11369 12 ago.
Goetz, C.G., 2011. The history of Parkinson's disease: early clinical descriptions and neurological therapies. Cold Spring Harb. Perspect. Med. 1 (1), 1–15 a008862, 1 set.
Gutteridge, J.M.C., Halliwell, B., 2018. Oxidative stress, redox stress or redox success? Biochem. Biophys. Res. Commun. 502 (2), 183–186 9 maio.
Hao, X.-M., et al., 2017. Neuroprotective effect of α-mangostin on mitochondrial dysfunction and α-synuclein aggregation in rotenone-induced model of Parkinson's disease in differentiated SH-SY5Y cells. J. Asian Nat. Prod. Res. 19 (8), 833–845 3 ago.
Hawlitschka, A., Wree, A., 2018. Experimental intrastriatal applications of botulinum neurotoxin-A: a review. Int. J. Mol. Sci. 19 (5) 1392 7 maio.
Kalia, L.V., Lang, A.E., 2015. Parkinson's disease. Lancet 386 (9996), 896–912 29 ago.
Karbowski, J., 2007. Global and regional brain metabolic scaling and its functional consequences. BMC Biol. 5 (1), 18 9 maio.
Krumschnabel, G., et al., 2015. Simultaneous high-resolution measurement of mitochondrial respiration and hydrogen peroxide production. Methods Mol. Biol. (Clifton, N.J.) 1264, 245–261 s.l: s.n.
Lehmensiek, V., et al., 2006. Dopamine transporter-mediated cytotoxicity of 6-hydroxydopamine in vitro depends on expression of mutant alpha-synucleins related to Parkinson's disease. Neurochem. Int. 48 (5), 329–340 abr.
Lemieux, H., et al., 2017. Impairment of mitochondrial respiratory function as an early biomarker of apoptosis induced by growth factor removal. bioRxiv(18 June), 151480.
Li, D.-W., et al., 2014. Guanosine exerts neuroprotective effects by reversing mitochondrial dysfunction in a cellular model of Parkinson's disease. Int. J. Mol. Med. 34 (5), 1358–1364 ago.
Lisowski, P., et al., 2018. Mitochondria and the dynamic control of stem cell homeostasis. EMBO Rep. 16, e45432 abr.
Lu, H., Forbes, R.A., Verma, A., 2002. Hypoxia-inducible factor 1 activation by aerobic glycolysis implicates the Warburg effect in carcinogenesis. J. Biol. Chem. 277 (26), 23111–23115 28 jun.
Magistretti, P.J., Allaman, I., 2018. Lactate in the brain: from metabolic end-product to signalling molecule. Nat. Rev. Neurosci. 19 (4), 235–249 8 abr.
Makrecka-Kuka, M., Krumschnabel, G., Gnaiger, E., 2015. High-resolution respirometry for simultaneous measurement of oxygen and hydrogen peroxide fluxes in permeabilized cells, tissue homogenate and isolated mitochondria. Biomolecules 5 (4), 1319–1338 29 jun.
Massari, C.M., et al., 2016. In vitro 6-hydroxydopamine-induced toxicity in striatal, cerebrocortical and hippocampal slices is attenuated by atorvastatin and MK-801.

Toxicol. Vitro 37, 162–168 dez.
Morroni, F., et al., 2018. Comparison of adaptive neuroprotective mechanisms of sulforaphane and its interconversion product erucin in *in vitro* and *in vivo* models of Parkinson's disease. J. Agric. Food Chem. 66 (January (4)), 856–865.
Pandya, J.D., et al., 2016. Age- and brain region-specific differences in mitochondrial bioenergetics in Brown Norway rats. Neurobiol. Aging 42 (1 june), 25–34.
Pesta, D., Gnaiger, E., 2011. High-resolution respirometry: OXPHOS protocols for human cells and permeabilized fibers from small biopsies of human muscle. Methods Mol. Biol. 810 (3 October), 25–58.
Qian, H., Yang, Y., 2009. Neuron differentiation and neuritogenesis stimulated by N-acetylcysteine (NAC). Acta Pharmacol. Sin. 30 (july 7), 907–912.
Radak, Z., et al., 2016. Physical exercise, reactive oxygen species and neuroprotection. Free Radic. Biol. Med. 98, 187–196 set.
Requejo-Aguilar, R., et al., 2014. PINK1 deficiency sustains cell proliferation by reprogramming glucose metabolism through HIF1. Nat. Commun. 5 (july), 4514–4524.
Requejo-Aguilar, R., Bolaños, J.P., 2016. Mitochondrial control of cell bioenergetics in Parkinson's disease. Free Radic. Biol. Med. 100 (november), 123–137.
Riederer, P., et al., 2018. Lateralisation in Parkinson disease. Cell Tissue Res. 14 abr.
Romuk, E.B., et al., 2017. The evaluation of the changes in enzymatic antioxidant reserves and lipid peroxidation in chosen parts of the brain in an animal model of Parkinson disease. Adv. Clin. Exp. Med. 26 (6), 953–959 set.
Sauerbeck, A., et al., 2011. Analysis of regional brain mitochondrial bioenergetics and susceptibility to mitochondrial inhibition utilizing a microplate based system. J. Neurosci. Methods 198 (1), 36–43 15 maio.
Schaar, C.E., et al., 2015. Mitochondrial and cytoplasmic ROS have opposing effects on lifespan. PLoS Genet. 11 (2), e1004972 11 fev.
Schöpf, B., et al., 2016. Oxidative phosphorylation and mitochondrial function differ between human prostate tissue and cultured cells. FEBS J. 283 (june 11), 2181–2196.
Simuni, T., et al., 2018. Longitudinal change of clinical and biological measures in early Parkinson's disease: parkinson's progression markers initiative cohort. Mov. Disord. 33 (March (5)), 771–782.
Singh, S., et al., 2010. Brain region specificity of 3-nitropropionic acid-induced vulnerability of neurons involves cytochrome c oxidase. Neurochem. Int. 57 (3), 297–305 out.
Teixeira, C.M., et al., 2018. Hippocampal 5-HT input regulates memory formation and schaffer collateral excitation. Neuron 98, 992–1004 8 maio.
Teves, J.M.Y., et al., 2018. Parkinson's disease skin fibroblasts display signature alterations in growth, redox homeostasis, mitochondrial function, and autophagy. Front. Neurosci. 11 (12 January), 737.
Trachootham, D., et al., 2008. Redox regulation of cell survival. Antioxid. Redox Signal. 10 (8), 1343–1374 ago.
Ungerstedt, U., 1968. 6-hydroxy-dopamine induced degeneration of central monoamine neurons. Eur. J. Pharmacol. 5 (1), 107–110 1 dez.
Vaishnavi, S.N., et al., 2010. Regional aerobic glycolysis in the human brain. Proc. Natl. Acad. Sci. 107 (41), 17757–17762 12 out.
Velazquez, R., et al., 2018. Acute tau knockdown in the hippocampus of adult mice causes learning and memory deficits. Aging Cell e12775 10 maio.
Wang, H.-L., et al., 2011. PARK6 PINK1 mutants are defective in maintaining mitochondrial membrane potential and inhibiting ROS formation of substantia nigra dopaminergic neurons. Biochim. Biophys. Acta 1812 (june 6), 674–684.
Wu, H.-M., et al., 2018. Mitochondrial DNA variants modulate genetic susceptibility to Parkinson's disease in Han Chinese. Neurobiol. Dis. 114 (june), 17–23.
Zheng, X., et al., 2018. A Comparative study for striatal-direct and -indirect pathway neurons to DA depletion-induced lesion in a PD rat model. Neurochem. Int. 16 abr.